

## Improvement Corrosion Resistance of Carbon Steel by Laser Surface Alloying within Nickel and Chromium Powders

Sami I.J. Alrubaiey and Hussein S.A. Fakhra  
University of Technology, Baghdad, Iraq

**Abstract:** Low carbon steel ST-37 had poor corrosion resistance in several environment. Therefore, Laser Surface Alloying (LSA) is done by using Ni and Cr powders. LSA is perform in two steps. The first, powder is stick on the surface by preplace method. The second step is laser processing to melt both powder and base metal to form an alloy on the surface. Solid state Nd:YAG laser pulse mode within specify laser parameter is used. Microstructure, surface alloy composition, corrosion behavior and regions depth after laser processing are study. Energy Dispersive Spectroscopy (EDS) optical microscope and potentialstate polarization technique are used in this study. Corrosion test is perfrom in 3.5% NaCl solution. Different corrosion parameters are studied ( $i_{corr}$ ,  $E_{corr}$ ,  $i_{passive}$ ,  $E_{passive}$ ,  $i_{transpassive}$ ,  $E_{transpassive}$ ). The aim of this research is to investigate the effect of laser alloy surface layer within different composition on corrosion behavior of steel. Different surface layer composition of Fe-Ni and Fe-Cr alloys are formed. The results show improving in corrosion resistance of steel due to form passive layer when the surface is alloying with Ni or Cr powders. The depth of melted and heat affected zones within Cr-powder is clearly more than Ni-powder samples.

**Key words:** Corrosion, steel, laser surface alloying, passivation, parameters, composition

---

### INTRODUCTION

The corrosion of metals is consider one of destructive processes. Alot of researches were done in different directions to develop a big range of engineering decisions. So, improvement corrosion resistance of metals is consider the most important problem in material application. Laser Surface Alloying (LSA) is consider one of new technologies in surface engineering field. The effects of LSA are to a change in surface composition and microstructure of the surface layer. Three zones are found after laser treatment, melted zone, Heat Affected Zone (HAZ) and base metal (Bartkowska *et al.*, 2016). The effect of changing scanning speed and laser power on hardness, wear resistance and microstructure was studied in research by Radziszewska and Kusinski (2008). Plain carbon steel and Ta powder were used in this research. The results showed that both hardness and wear resistance were improved. Different solidification modes were put due to different microstructures which formed at each laser parameter. Proper selection of alloying additives and laser process parameters are allowed to obtain adequate surface layer with new properties. Whereas these properties are difficult to obtain within traditional methods. Localized heating can performs, minimize HAZ region and vacume is not required. In addition, little thermal penetration very high heating and

cooling rates (Bartkowska *et al.*, 2016). Four different substrate alloys were used in research (Kwok and Wong, 2010). Mild steel, austenitic stainless steel, aluminum alloy and brass with Fe Cr Mo Mn WCB powder (Nanosteel SHS 717). Microstructure, sliding wear and corrosion behavior were studied. The results explained that all of laser-alloyed samples showed no passivation in 3.5% NaCl solution at 23°C. Except laser-alloyed brass, the corrosion resistance of laser alloyed of rest types were deteriorated after LSA. Hardness and sliding wear resistance also improved after laser surface alloying processing. Steel is the most important alloy used in material engineering application but due to its limit corrosion resistance, different surface modification methods are used to improve it. These modification included all types of surface treatments and coatings. The research by Abdolahi *et al.* (2011) to produce a thick and integrated surface layer of iron aluminides on the surface of a low carbon steel sheet. The corrosion resistance of the coated samples was evaluated by activation polarization and Tafel methods. The results showed that laser processing of the aluminized steel led to a considerable increase in its corrosion resistance compared to both uncoated and merely aluminized materials. Laser surface alloying involves melting surface area (locally) of base material and of researcher material brought into the area. Different alloying element can be used. The added

alloying elements will form an alloy within base material during melting with laser. Alloying elements that will be melted on the base material are commonly presented as metallic powders. Different methods are used to deposited of powder in the area of laser processing (Turcan *et al.*, 2013). The aim of this research is to develop the corrosion resistance of low carbon steel by LSA process, using nickel and chromium powders.

## MATERIALS AND METHODS

Samples of low carbon steel (ST-37) are used in this research. The chemical composition of the used samples show in Table 1. The samples firstly grained within SiC study's (180, 320, 600, 1000, 3000) and polished within Alumina (Al<sub>2</sub>O<sub>3</sub>) solution then etched in nital solution to investigate the microstructure of low carbon steel. The microstructure were examined by using optical microscope. Pure nickel and chromium powders are used within purity 99.7, 99.51%, respectively. Average powders particle size are 45 μm. The powders are supply from CPNH company China.

**Samples preparation for LSA process:** As received plate of low carbon steel ST-37 is machined into dimensions (30×30) mm with 6 mm thickness by using wire cut machine model charmilles robofil 400. Samples are then grinding within graining machine for primary graining then with SiC study grade 180 for final grinding. Samples are then clean with Ethanol and Aceton in order to remove oxide layers and contamination.

**Powder preplace method:** Two samples groups were prepared for preplacing process. First group is within pure Ni-powder and the second one is within pure Cr-powder. In order to do preplaced method, powder is at first mix with Sodium silicate solution. This solution prepare by mixing 10 mL of distil water with 4 mL of Sodium silicate and then mix within 3 g of powder. This mixture is then put on the samples within the required thickness and then heated on oven to 100°C in order remove water and mounted powder on the samples.

**Laser surface alloying processing:** Laser surface alloying processing was performed in Iranian National Center for Laser Science and Technology (INLC), Tahrán, Iran. The laser used in this study is solid state, pulse mode with the main technical parameters wavelength,  $\lambda = 1.0641 \mu\text{m}$ , Laser frequency (pulse repetition rate) = 1-200 Hz, pulse energy, E = 1-50 Joules, pulse width = 0.2-20 msec. Pulse peak power = up to 10 kW, Model IQL-20. Specify laser paratmeter are used within this study. Pulse

Table 1: Chemical composition of used steel ST 37

C (%)	Mn (%)	Cr (%)	Ni (%)	V (%)	Al (%)	Cu (%)	Fe (%)
0.131	0.432	0.010	0.032	0.002	0.038	0.020	Bal

duration = 8 msec, Speed of laser = 6.2 mm/sec, Frequency = 20 Hz, average power = 280 Watt, pulse energy = power/frequency = 280/20 = 14 Joule, peak power = energy/pulse duration = 14/8 = 1.75 kW, Following Ar pure 99.999 = 30 L/min coaxial, Defocus distance = 6 mm, Overlap between the center of tracks = 30% and Laser beam diameter = 0.114 cm. A model 5000 W, LP Ophir power meter and LA 300 W-LP Joule meter were used to measure mean power and pulse energy. Laser equipment is consisting of laser power generator, cooling unit and a movement table.

**Metallography and microstructural examination:** Optical Microscope (OM) and Energy Dispersive Spectroscopy (EDS) were used to examine the microstructure and chemical composition before and after laser surface alloying processing.

**Optical Microscope (OM):** Optical microscope type (A. Kruss Optronic GmbH) is used to study the microstructure before and after LSA process.

**Energy Dispersive Spectrometer (EDS):** EDS device is used in order to check the chemical composition of the surface after laser alloy process this device is usually connected to scanning electron microscope SEM. The device that is used in this test is TESCAN Model Vega made in Czech Republic.

**Preparing samples for corrosion test:** In order to perform corrosion test for laser alloyed samples these samples are mounting at first, so that, only surface area will attack by corrosion electrolyte. The samples are prepared by cutting them to (10×10 mm) by using EDM wire cut machine. Samples then mounted by resin. A copper wire must be connected to the sample before doing mounting process.

**Corrosion test:** The corrosion behavior was studied by Tafel extrapolation technique, using potentialstate type MLAB 200. The polarization cell consists of working electrode (low carbon steel) reference electrode (Calomel). The lugging probe was kept at distance of 1 mm from the surface of working electrode and platinum (Auxiliary electrode). These electrodes were connected to a computerized potentiostat (bank electronics 200-German made). The solution of corrosion test was 3.5% NaCl solution. The corrosion test and microstructure examination are performed before and after LSM treatment for each value of laser energy.

**RESULTS AND DISCUSSION**

The microstructure of as received low carbon steel is consist of ferrite and pearlite as shown in Fig. 1. Table 2 show EDS results after LSA processing. The difference in chemical composition is due to the difference in powder preplacing thickness.

**Dimensions of the melted and HAZ regions:** Different melted pool and HAZ depth are due to different powders that use during LSA process (Fig. 2). The different in melted zone depth is due to different absorption of laser beam between Ni and Cr powders. The absorptivity of Ni, Cr and steel are 0.221, 0.423, 0.35, respectively for Nd.YAG laser (Johnson and Christy, 1974). Figure 3 and 4 show three zones after LSA process. Table 3 shows the dimensions of melted and HAZ regions.

The results show that depth of both melted and HAZ regions for Cr-powder bigger than Ni-powder. This is due to higher absorptivity of Cr for laser energy than Ni. Therefore, bigger amount of laser energy will be absorbed and cause more increasing of temperature.

**Corrosion results:** The alloying element Ni and Cr are implemented on steel surface by LSA process. Corrosion test is done to study the effect of surface alloying element. The corrosion parameters studied are ( $i_{corr}$ ,  $E_{corr}$ ,  $i_{passive}$ ,  $E_{passive}$ ,  $i_{transpassive}$ ,  $E_{transpassive}$ ). As received corrosion parameters  $i_{corr}$ ,  $E_{corr}$ , corrosion rate are  $2.3 \times 10^{-2}$  mA/cm<sup>2</sup>, 630.7 mV,  $1.0843 \times 10^{-2}$  mpy, respectively. Figure 4 show polarization curves of as received steel ST-37.

**Corrosion result after laser surface alloying within nickel powder:** When steel surface is implemented by Ni, there are some improvement of corrosion resistance. Ni<sup>-1</sup> sample corrosion parameters  $i_{corr}$ ,  $E_{corr}$ , corrosion rate are changed to  $2.4 \times 10^{-3}$  mA/cm<sup>2</sup>, -600 mV,  $1.0900 \times 10^{-3}$  mpy, respectively. Whereas Ni<sup>-2</sup> sample corrosion parameters  $i_{corr}$ ,  $E_{corr}$ , corrosion rate are change to  $7.8 \times 10^{-3}$  mA/cm<sup>2</sup>, 565.5 mV,  $3.5425 \times 10^{-3}$  mpy, respectively. Ni also affected the behavior of polarization curves. In research, Nabeel Alharthi *et al.* (2017) reported that present of Ni in steel could change the behavior of anodic polarization from active to passive behavior. Passivation zone appears in sample which implemented by Ni. The thickness of the Ni-powder layer had an effect on corrosion behavior. When the thickness of Ni-powder layer is 320  $\mu$ m, average Ni% is 20.33. Average laser alloyed thickness is 186.38  $\mu$ m in Ni<sup>-2</sup> sample. Whereas, the thickness of the Ni-powder layer increase to 350  $\mu$ m, average Ni% is 17.46. Average laser alloyed thickness is 230.51  $\mu$ m in Ni<sup>-1</sup> sample. The results show that  $i_{passive}$  is equal to  $2.0 \times 10^{-2}$  mA/cm<sup>2</sup> in Ni<sup>-1</sup>

Table 2: EDS results after LSA processing

Samples	At the top of the center	At the bottom of the center	At the top of the overlap	At the bottom of the overlap
Ni <sup>-1</sup>	18.94% Ni	16.00% Ni	18.8% Ni	16.10% Ni
Ni <sup>-2</sup>	21.66% Ni	17.69% Ni	20.4% Ni	21.57% Ni
Cr <sup>-1</sup>	16.88% Cr	15.68% Cr	13.1% Cr	15.42% Cr
Cr <sup>-2</sup>	6.3% Cr	5.53% Cr	6.23% Cr	6.46% Cr

Table 3: The dimensions of melted and HAZ regions

Sample	Average Melted zone depth ( $\mu$ m)	Average HAZ depth ( $\mu$ m)
LSA within Ni-powder	272.24	85.310
LSA within Cr-powder	350.02	95.401

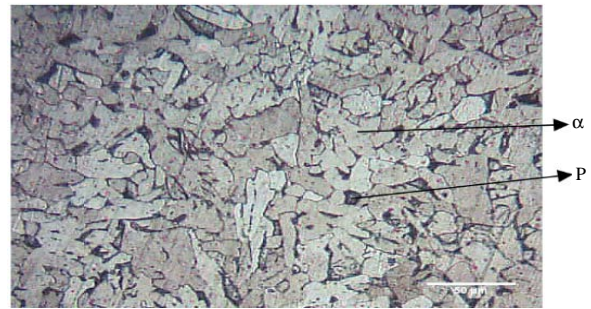


Fig. 1: Microstructure of as received low carbon steel ST-37



Fig. 2: Laser surface alloying zones within Nickel powder

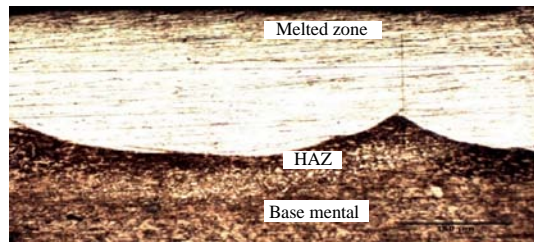


Fig. 3: Laser surface alloying within Chromium powder

sample. While it increase to  $3.6 \times 10^{-2}$  mA/cm<sup>2</sup> for Ni<sup>-2</sup> sample. This is due to stability of Ni-oxide (Cottis *et al.*, 2010). Ni-oxide formed at lower Ni% is more stable and formed easier than at higher Ni%. This layer is break down at lower current density for 17.46% Ni. The value of  $i_{transpassive}$  is equal to  $1.9 \times 10^{-1}$  mA/cm<sup>2</sup>. Whereas it decrease to  $1.5 \times 10^{-1}$  mA/cm<sup>2</sup> at higher Ni%. Passive layer is stable for large range of potential at low Ni%. The difference

between  $E_{\text{passive}}$  and  $E_{\text{transpassive}}$  is equal to 272.6 mV. Whereas its 152.4 mV at higher Ni content. Figure 5 and 6 show the polarization curves for  $\text{Ni}^{-1}$  and  $\text{Ni}^{-2}$  samples. Table 4 show the corrosion parameters for as received,  $\text{Ni}^{-1}$  and  $\text{Ni}^{-2}$  samples.

**Corrosion result after laser surface alloying within chromium powder:** When steel surface is implemented by Cr there are some improvement of corrosion resistance.  $\text{Cr}^{-1}$  sample corrosion parameters  $i_{\text{corr}}$ ,  $E_{\text{corr}}$ , corrosion rate are change to  $1.1 \times 10^{-2} \text{ mA/cm}^2$ , -590.2 mV,  $5.3868 \times 10^{-3} \text{ mpy}$ , respectively. Whereas  $\text{Cr}^{-2}$  sample corrosion

$E_{\text{corr}}$ , corrosion rate are change to  $3.6 \times 10^{-2} \text{ mA/cm}^2$ , 544.4 mV,  $1.6730 \times 10^{-2} \text{ mpy}$ , respectively. Cr also has observably affects on the behavior of polarization curve. In research by Kirchheim *et al.* (1989) reported that present of Cr in steel could change the behavior of anodic polarization from active to passive behavior. Passivation zone appears in samples which implemented by Cr. The thickness of the Cr-powder layer had an effect on corrosion behavior. When the thickness of Cr-powder layer is 270  $\mu\text{m}$ , average Cr% is 6.13. Average laser alloyed thickness is 243.9  $\mu\text{m}$  in  $\text{Cr}^{-2}$  sample. Whereas, the thickness of the Cr-powder layer increase to 450  $\mu\text{m}$ , average Cr% is 15.27. Average laser alloyed thickness is 314.42  $\mu\text{m}$  in  $\text{Cr}^{-1}$  sample. The results show that  $i_{\text{passive}}$  is equal to  $5.0 \times 10^{-2} \text{ mA/cm}^2$  in  $\text{Cr}^{-1}$  sample. While it increase to  $1.6 \times 10^{-1} \text{ mA/cm}^2$  for  $\text{Cr}^{-2}$  sample. This is due to stability of Cr-oxide. Cr-oxide that formed at higher Cr% is more stable and formed easier than at low Cr%. This layer is break down at lower current density for 15.27% Cr. The value of  $i_{\text{transpassive}}$  is equal to  $3.5 \times 10^{-1} \text{ mA/cm}^2$ . Whereas it increase to  $3.5 \times 10^{-1} \text{ mA/cm}^2$  at lower Cr%. Passive layer is stable for large range of potential at higher Cr%. The difference between  $E_{\text{passive}}$  and  $E_{\text{transpassive}}$  is equal to 273.9 mV. Whereas its 215.8 mV at lower Cr content. Figure 7 and 8 show the polarization curves for  $\text{Cr}^{-1}$  and  $\text{Cr}^{-2}$  samples.

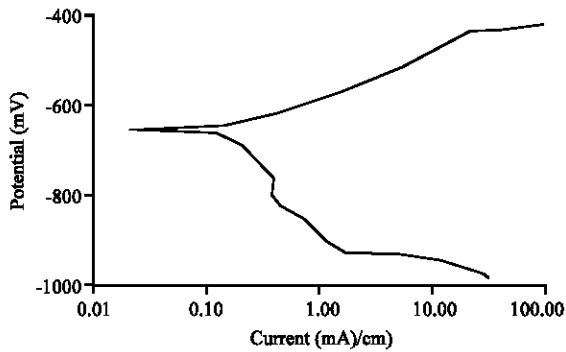


Fig. 4: Polarization curve of as received steel ST-37

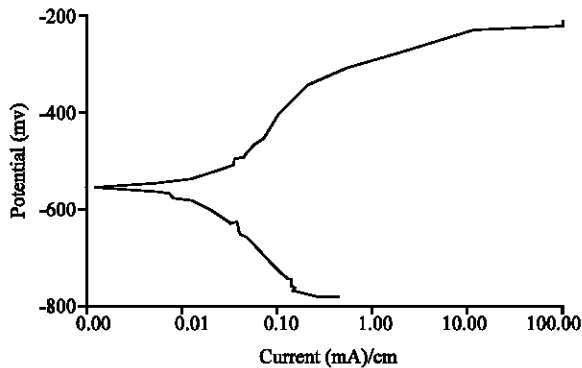


Fig. 5: Polarization curve of  $\text{Ni}^{-1}$  sample

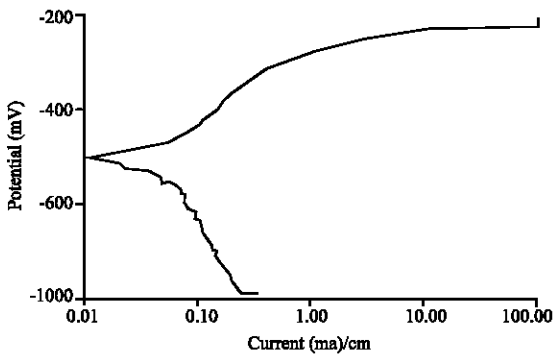


Fig. 6: Polarization curve of  $\text{Cr}^{-1}$  sample parameters  $i_{\text{corr}}$

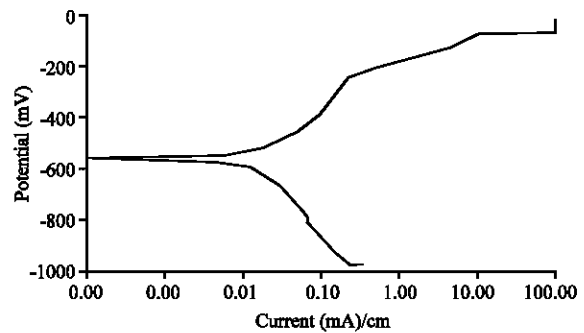


Fig. 7: Polarization curve of  $\text{Ni}^{-2}$  sample

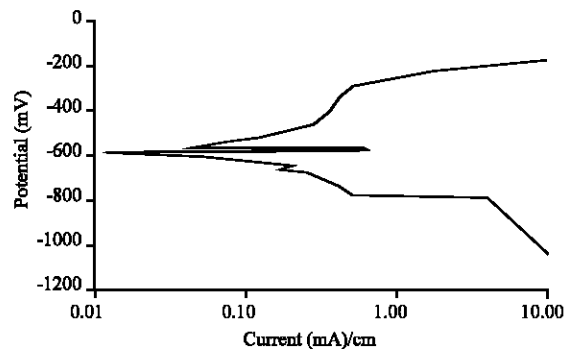


Fig. 8: Polarization curve of  $\text{Cr}^{-2}$  sample

Table 4: Corrosion parameters of Ni laser processing samples

Sample	$E_{corr}$	$i_{corr}$	$E_{passive}$	$I_{passive}$	$E_{transpassive}$	$i_{transpassive}$	$\Delta E (E_{tran.}-E_{pass})$	Corrosion rate (mpy)
As received	-630.7	$2.3 \times 10^{-2}$	-	-	-	-	-	$1.0843 \times 10^{-2}$
Ni <sup>-1</sup>	-600.0	$2.4 \times 10^{-3}$	-529.4	$2.0 \times 10^{-2}$	-256.8	$1.9 \times 10^{-1}$	272.6	$1.0900 \times 10^{-3}$
Ni <sup>-2</sup>	-565.5	$7.8 \times 10^{-3}$	-440.2	$3.6 \times 10^{-2}$	-287.8	$1.5 \times 10^{-1}$	152.4	$3.5425 \times 10^{-3}$

Table 5: Corrosion parameters of Cr laser processing samples

Sample	$E_{corr}$	$i_{corr}$	$E_{passive}$	$I_{passive}$	$E_{transpassive}$	$i_{transpassive}$	$\Delta E (E_{tran.}-E_{pit})$	Corrosion rate (mpy)
As received	-630.7	$2.3 \times 10^{-2}$	-	-	-	-	-	$1.0843 \times 10^{-2}$
Cr <sup>-1</sup>	-590.2	$1.1 \times 10^{-2}$	-492.0	$5.0 \times 10^{-2}$	-218.1	$3.5 \times 10^{-1}$	273.9	$5.3868 \times 10^{-3}$
Cr <sup>-2</sup>	-544.4	$3.6 \times 10^{-2}$	-484.9	$1.6 \times 10^{-1}$	-269.1	$7.0 \times 10^{-1}$	215.8	$1.6730 \times 10^{-2}$

Table 5 shows the corrosion parameters for as received, Cr<sup>-1</sup> and Cr<sup>-2</sup> samples. A chromium oxide layer act as a barrier against ions diffusion through metal surface. The polarization behavior changes of Fe-Cr alloy is due to combination of chromium oxide (Cr<sub>2</sub>O<sub>3</sub>) and ((Fe, Cr)<sub>2</sub>O<sub>3</sub>) at the surface. These oxide films act as a protective layer against corrosion due to its low diffusion constants for metal ions and oxygen (Abdolahi *et al.*, 2014; Cottis *et al.*, 2010; Donik and Aleksandra, 2014).

**CONCLUSION**

- Improvement of corrosion resistance of low carbon steel after LSA processing
- With increasing Ni content, cause decreasing in corrosion resistance
- With increasing Cr content, cause increasing in corrosion resistance
- Passivation layer appear after LSA
- The depth of melted and heat affected zones within Cr-powder is clearly more than Ni-powder samples

**REFERENCES**

Abdolahi, B., H.R. Shahverdi, M.J. Torkamany and M. Emami, 2011. Improvement of the corrosion behavior of low carbon steel by laser surface alloying. *Appl. Surf. Sci.*, 257: 9921-9924.

Alharthi, N., E.S.M. Sherif, H.S. Abdo and S.Z. El-Abedin, 2017. Effect of nickel content on the corrosion resistance of iron-nickel alloys in concentrated hydrochloric acid pickling solutions. *Adv. Mater. Sci. Eng.*, 2017: 1-8.

Bartkowska, A., D. Przystacki and T. Chwalczuk, 2016. Microstructure, phase composition and corrosion resistance of Ni<sub>2</sub>O<sub>3</sub> coatings produced using laser alloying method. *Arch. Mech. Technol. Mater.*, 36: 23-29.

Cottis, R.A., M.J. Graham, R. Lindsay, S.B. Lyon and J.A. Richardson *et al.*, 2010. Shreir's Corrosion. 4th Edn., Elsevier, Amsterdam, Netherlands.

Donik, C. and K. Aleksandra, 2014. Comparison of the corrosion behavior of austenitic stainless steel in seawater and 3.5%NaCl solution. *Mater. Technol.*, 48: 937-942.

Johnson, P.B. and R.W. Christy, 1974. Optical constants of transition metals: Ti, V, CR, mn, FE, CO, NI and PD. *Phys. Rev. B*, 9: 5056-5070.

Kirchheim, R., B. Heine, H. Fischmeister, S. Hofmann and H. Knotte *et al.*, 1989. The passivity of Iron-chromium alloy. *Corros. Sci.*, 29: 899-917.

Kwok, C.T. and P.K. Wong, 2010. Laser surface alloying of various engineering alloys for sliding wear and corrosion resistance. *J. Laser Micro. Nanoeng.*, 5: 90-96.

Radziszewska, A. and J. Kusinski, 2008. Laser alloying of the plain carbon steel surface layer. *Arch. Foundry Eng.*, 8: 175-179.

Turcan, O., D.C. Comeaga, O. Dontu and I. Voiculescu, 2013. Improvement of low carbon steel ST37-2 by laser surface alloying with metallic powders. *Adv. Mater. Res.*, 816: 250-254.